Journal of Saudi Chemical Society (2019) **23**, 171–181

King Saud University

Journal of Saudi Chemical Society

www.ksu.edu.sa
www.sciencedirect.com

ORIGINAL ARTICLE

Growth of Wall-controlled MWCNTs by Magnetic Field Assisted Arc Discharge Plasma

M.S. Roslan [a,b,*], K.T. Chaudhary [b], N. Doylend [c], A. Agam [a], R. Kamarulzaman [a], Z. Haider [b], E. Mazalan [b], J. Ali [b]

[a] *Universiti Tun Hussein Onn Malaysia, 86400, Parit Raja, Batu Pahat, Johor Darul Takzim, Malaysia*
[b] *Laser Center, Ibnu Sina Institute for Scientific and Industrial Research (ISI-SIR), Universiti Teknologi Malaysia, 81310, Skudai, Johor Bahru, Malaysia*
[c] *Centre for Renewable Energy Systems Technology (CREST), School of Electronic, Electrical, and Systems Engineering, Loughborough University, Loughborough, Leicestershire LE11 3TU, United Kingdom*

Received 21 March 2018; revised 5 June 2018; accepted 9 June 2018
Available online 21 June 2018

KEYWORDS

Arc discharge;
Nanostructured;
Multiwalled Carbon Nanotubes (MWCNTs)

Abstract Carbon nanotubes have long attracted great scientific interest because of their simplicity, ease of synthesis and unique properties. The novel properties of nanostructured carbon nanotubes including its high surface area, stiffness, tensile strength, thermal and electrical properties which become suitable for the application in the fields of energy storage, hydrogen storage, electrochemical supercapacitor, field-emitting devices, transistors, nanoprobes and sensors, composite material, templates, etc. In this study, carbon nanotubes were synthesized through arc discharge plasma with two different configurations, transverse and axial field, applied across arc plasma synthesis process to enable a much rapid rate growing of tubular carbon multi-walled carbon nanotubes (MWCNTs). TEM, FESEM, RAMAN, FTIR and XRD were used to investigate the morphology and structural evolution of the MWCNT samples produced with different synthesis environment. Introduction of magnetic field during the MWCNTs synthesized through arc discharge plasma technique has also been found to enhance the carbon nanotube growth, increase the high aspect ratio and its chemical stability, and shows potential for regulating the number of walls formed.

1. Introduction

Carbon nanotube is one of carbon allotropes with extraordinary electrical, thermal and mechanical properties [1]. The tubular shape of the carbon nanotube is built up by covalent bonds with hexagonal miniature, giving them high tensile strength with Young's Modulus potentially reaching 1 TPa [2], inversely proportional to diameter and dependent on chiral angles. There are several techniques used to synthesize carbon

* Corresponding author at: Universiti Tun Hussein Onn Malaysia, 86400, Parit Raja, Batu Pahat, Johor Darul Takzim, Malaysia.
E-mail address: sufi@uthm.edu.my (M.S. Roslan).
Peer review under responsibility of King Saud University.

Production and hosting by Elsevier

https://doi.org/10.1016/j.jscs.2018.06.003
1319-6103

nanotubes including laser ablation [3], chemical vapor deposition (CVD) [4], plasma enhanced CVD [5], thermal growth [6], and arc discharge plasma [7,8].

Arc discharge plasma is one of the most efficient techniques to grow MWCNTs [9]. However, this technique is facing major issues such as the growth of controlled CNT structures and the presence of impurities including graphene and nanohorn [10]. The arc discharge process to grow MWCNTs depends on applied conditions including background gas [11–13] ambient pressure [14,15], mechanism of electrode separation [16], and amount of current flow [17]. The selection of ambient conditions to synthesize carbon nanotube is crucial in order to grow high quality MWCNTs for specified applications. By maintaining appropriate experimental conditions, high density and well aligned MWCNTs could be grown by incorporating magnetic fields into the arc discharge plasma technique [18].

On the other hand, as presented in the majority of reports, MWCNTs can grow even without the support of a catalyst. Primarily, the alteration of experimental parameters results in different plasma conditions and spatial distribution, as well as carbon nucleation and growth in the time and space domain. Ambient conditions have a great influence on the diameter of carbon nanotube [19]. Ambient pressure plays a critical role in the arc synthesis process since the mean free path is easily affected by background plasma pressure. Carbon nanotubes grow in extreme high temperature media. In this case, arc discharge plasma is an efficient technique to grow carbon nanotubes as the carbon plasma is enriched with carbon ions that support nucleation of carbon nanotube structure [20]. However, the motion of charged particles resulting from the arc discharge plasma is certainly affected by magnetic field and hence can potentially enhance the growth of carbon nanotube [21]. Through applying magnetic field, the lifetime of electrons in target vicinity certainly can be increased [22]. This can be realized by adding permanent magnet behind the cathode target. Therefore, the fundamental understanding of the relationship between arc plasma and growth process of carbon nanotube is an important research objective. Hence, this study investigates the effect of transverse and axial magnetic fields on the growth of MWCNT structure.

2. Experimental

Vacuum chambers provide controlled conditions for experimental processes to take place. In this study, a stainless-steel chamber was used to synthesis MWCNTs as depicted in Fig. 1. The chamber consists of four main ports; two ports were used for electrode connections, the others were used for the motor connection and viewing port. A Thorlab MTZ-25 motorized stage with a 25 mm maximum displacement and precision up to ± 5 nm was used to control the movement of the anode and therefore vary the anode–cathode separation. The anode and cathode consisted of high purity graphite of diameter 9 mm and 12 mm respectively. The anode featured an inner hole of diameter 5.5 mm. This ensures smaller interaction area on the anode side relative to the cathode side in order to create diffusive arc phenomena [23]. This will enhance anode erosion and increase cathode deposition therefore increase formation of CNTs. After the transverse/axial magnetic field was established by putting permanent magnet NdFeB in between electrodes until reach field strength 30 mT measured by Teslameter, within the vacuum chamber, the chamber was evacuated with rotary and diffusion pumps until the base pressure of 10^{-5} mbar was reached. The butterfly valve connected to the vacuum pump and chamber was then used to control the ambient environment pressure up to required value, which was then maintained throughout the arc discharge process.

An arc plasma was generated across the anode and cathode gap by applying the touch ignition technique at potential 12 V and current flow 70 A. The Teflon anode stand was attached to the motorized stage while the cathode stand was fixed on the opposite site. The arc discharge experiments were carried by first making contact between two graphite electrodes. The anode and cathode were then slowly separated (to approximately 0.05 mm) to allow ignition of arc plasma. The movement was controlled by motorized stage at a speed of 2.5 mm/s to adjust the anode position. Following arc plasma ignition, the electrode separation was maintained at approximately 1 mm by moving the anode forward to compensate for the mass loss by deposition on the cathode surface. The experiment was repeated several times to collect sufficient samples for further microscopic and spectroscopic analyses including electron microscope (FESEM and TEM), Raman spectroscopy, X-Ray diffraction (XRD) and Fourier transform Infrared (FTIR) spectroscopy. Result of the samples collected and analyzed is discussed in the next section.

3. Morphology and structural evolution

MWCNTs grown by arc discharge plasma techniques are perceived to have high quality nanotube structure with predominantly straight tube growth. As observed by TEM images, MWCNT samples prepared in an air environment at ambient pressures 10^{-2}, 1 and 10^{2} mbar in the absence of external magnetic fields mostly grow as a mixture of amorphous carbon and carbon nano-onion. At an ambient pressure of 10^{-2} mbar, long MWCNT structures reach several micrometers in length and nano-onion is observed. At a pressure of 1 mbar, MWCNTs grow with fine structure and fewer impurities. The tubes were observed to grow up to few hundreds nanometers only. Less nano-onion growth was observed under this condition. In areas where MWCNTs mostly formed, smaller amounts of graphene stakes and CNT bundles were observed, while in areas where graphene mostly formed, much less nanotube growth was observed. At a pressure of 10^{2} mbar, results show MWCNTs grown in a mixture with other carbon nanostructures such as graphene, carbon nano-onion, and amorphous carbon. Branched nanotubes are also commonly found under these conditions. Fig. 2(a) shows a TEM image of MWCNT obtained by discharge in an air environment under an axial magnetic field at an ambient pressure of 10^{-2} mbar. The image clearly shows straight MWCNTs with a small inner diameter of 2.20 nm and an outer diameter of 12.68 nm with an interspacing layer of 0.34 nm. As the ambient pressure increased further, changes to the inner-tube size and diameter are clearly evident (Fig. 2(b) and (c)). The variation of tube dimensions including length and diameter based on direct measurement from TEM micrograph using software ImageJ is shown in Figs. 3–4. The alteration of tube dimensions according to the changes of ambient pressure and magnetic field configuration is also discussed.

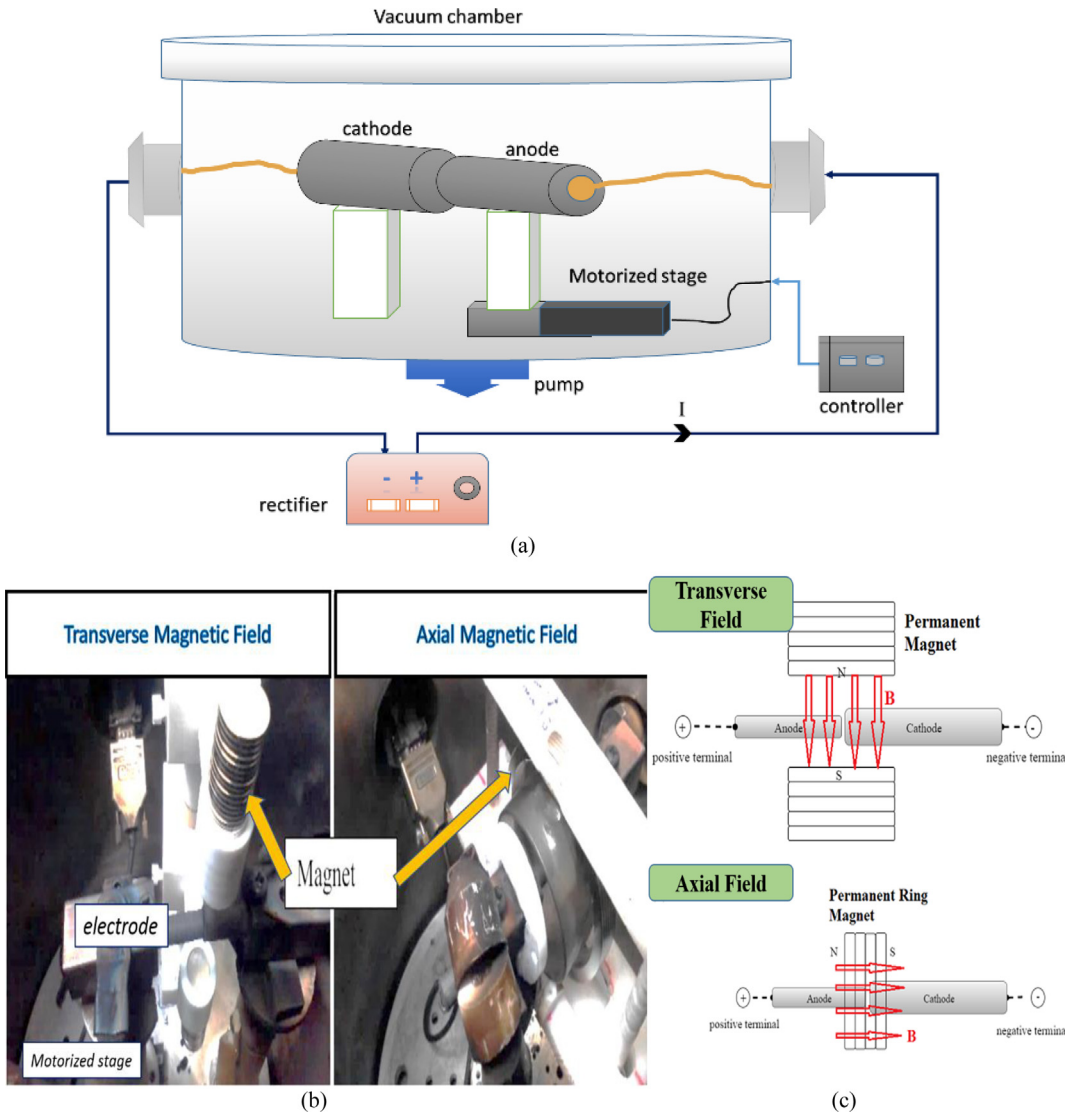

Fig. 1 (a) Schematic of experimental setup for synthesis of MWCNTs and (b) and (c) axial and transverse magnetic configuration.

Fig. 3 shows the trend of average CNT diameter synthesized under different ambient pressures and magnetic field configuration. The magnetic field strength was maintained at 30 mT. The trend shows that carbon nanotubes grow with outer diameters in the range 16–20 nm in the absence of an applied magnetic field, B_0. On the other hand, results show the diameter of CNT decreased to approximately 12–14 nm with an applied transverse magnetic field, B_T. Further reduction in CNT diameters was observed with an applied axial magnetic field effect where tube diameter noticeably reduced to approximately 10–12 nm. Ambient pressure also significantly affects the growth of the carbon nanotube structure. The trend shows that at low ambient pressure (10^{-2} mbar) tube diameter is larger, average 19.21 nm, than at higher ambient pressure (10^{2} mbar), average 15.83 nm, in absence of magnetic field.

The reduction in tube diameter may occur as a result of increases in plasma pressure and the effect of external magnetic field on the arc plasma [24]. The effect is more prominent under axial magnetic fields compared with transverse fields as the direction of magnetic field lines follow the flow direction of carbon ions toward the anode terminal. This effect inevitably increases the pressure of plasma thus limiting tube growth in the radial direction.

Fig. 4 shows the trend of average CNT length when grown under different magnetic configuration in different ambient pressures from 10^{-2} to 10^{2} mbar. The graph shows that synthesis in the absence of magnetic field promotes the growth of long carbon nanotube structures with an average length of 650 nm. When a magnetic field is applied across the arc discharge plasma, results show that the CNT length decreases by approximately 100 nm. However, ambient pressures of 1 and 10^{2} mbar result in longer tube structure, approximately 550 nm, under the influence of the transverse magnetic field, while the axial magnetic field results in tube structure with an average length of approximately 500 nm.

Fig. 5 shows the aspect ratio (length/diameter) of carbon nanotubes synthesized in an air environment under different magnetic configurations and ambient pressures. The trend reveals that, in the absence of an applied magnetic field, low aspect ratio CNTs were obtained in this experiment.

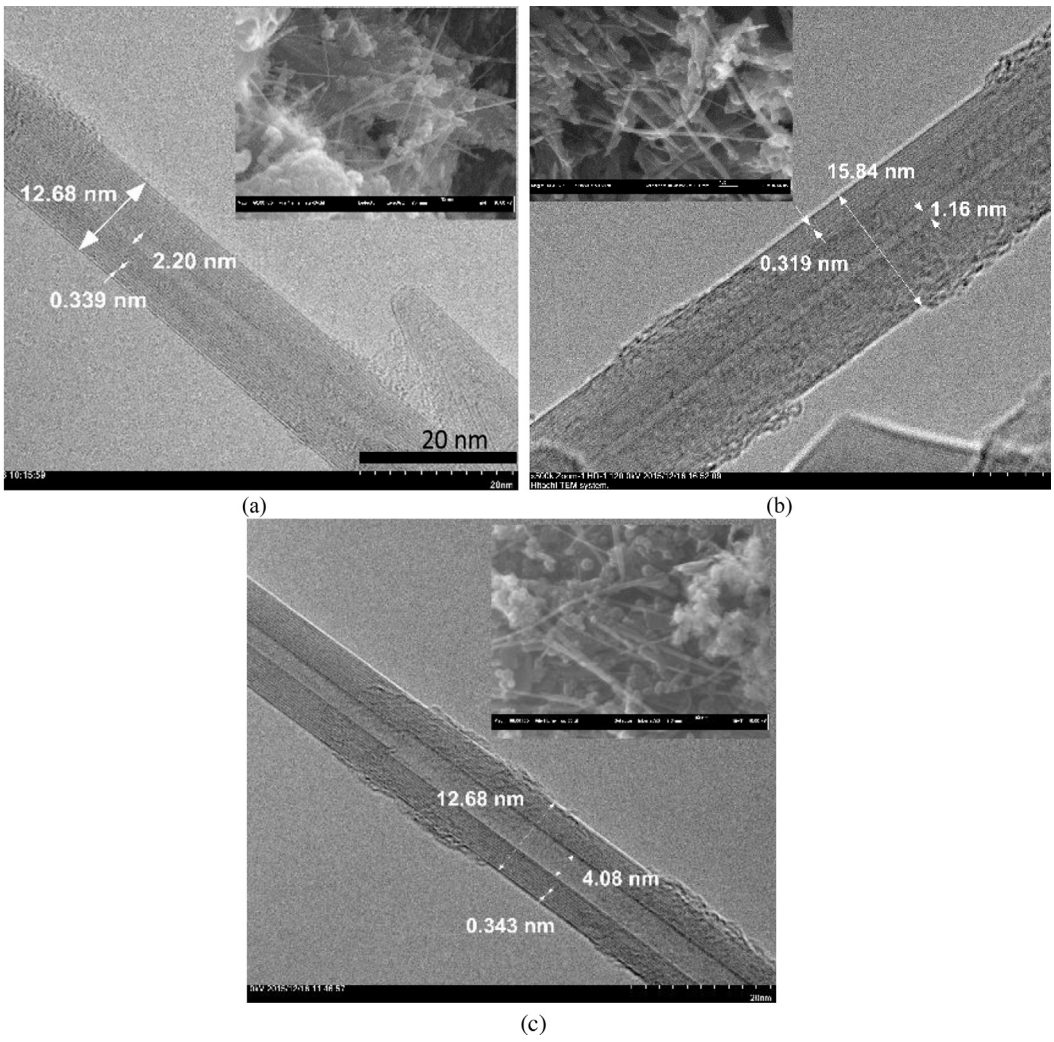

Fig. 2 TEM micrograph of MWCNT obtained under axial magnetic field configuration at ambient pressure (a) 10^{-2} mbar (b) 1 mbar and (c) 10^{2} mbar (inset shows the FESEM image of MWCNTs under similar experimental conditions).

Significant changes can be observed as the aspect ratio of CNTs increased with applied transverse and axial magnetic fields at ambient pressures of 1 and 10^{2} mbar. Moreover, the highest aspect ratio of CNTs observed in this experiment under the influence of axial magnetic field at an ambient pressure of 10^{-2} mbar indicates substantial long tube structure growth in the specified condition.

4. Raman analysis

Raman spectroscopy is a powerful tool to characterize carbon nanotubes. Fig. 6 shows the Raman spectra obtained for CNTs synthesized under different ambient pressures from 10^{-2} to 10^{2} mbar with different magnetic configuration, transverse (B_T) and axial (B_A). The Raman spectroscopy analysis was carried out by exciting samples using argon-ion laser at a wavelength of 514.5 nm. The spectra show Raman shift for wavenumbers ranging from 1200 cm^{-1} to 1800 cm^{-1}, and depict two prominent peaks represented as D band (1350 cm^{-1}) and G band (1580 cm^{-1}). The G band represents vibration in the plane of sp^2 in the graphitic structure while D band represents the vibration out of the plane of graphitic structure [25]. The increase in D band intensity indicates the phenomena of structural imperfection in the carbon nanotube structure. On the other hand, the increase in the G band peak intensity infers increase in ordered graphitic structure of carbon. Conversely, a weak G band represents less ordered tube structure and the increase in amorphous carbon. Referring to the Raman spectra of CNTs grown in absence of magnetic field effect, B_0 shows improvement in graphitic structure as ambient pressure increases from 10^{-2} to 10^{2} mbar indicated by the high rise in G band with increasing ambient pressure. On other hand, improvement in graphitic structure is observed at low ambient pressure of 10^{-2} mbar as shown in Fig. 6 for the CNTs samples prepared under transverse magnetic field, B_T. Under the influence of axial magnetic field B_A, a high rise in graphitic CNT structure was observed under ambient pressures of 10^{-1} and 1 mbar.

Table 1 summarizes the Raman features for different conditions applied to synthesize CNTs under the influence of an external magnetic field. The G band in sp^2 nanocarbon is affected by strain on the structure [26]. Biaxial tensile stress

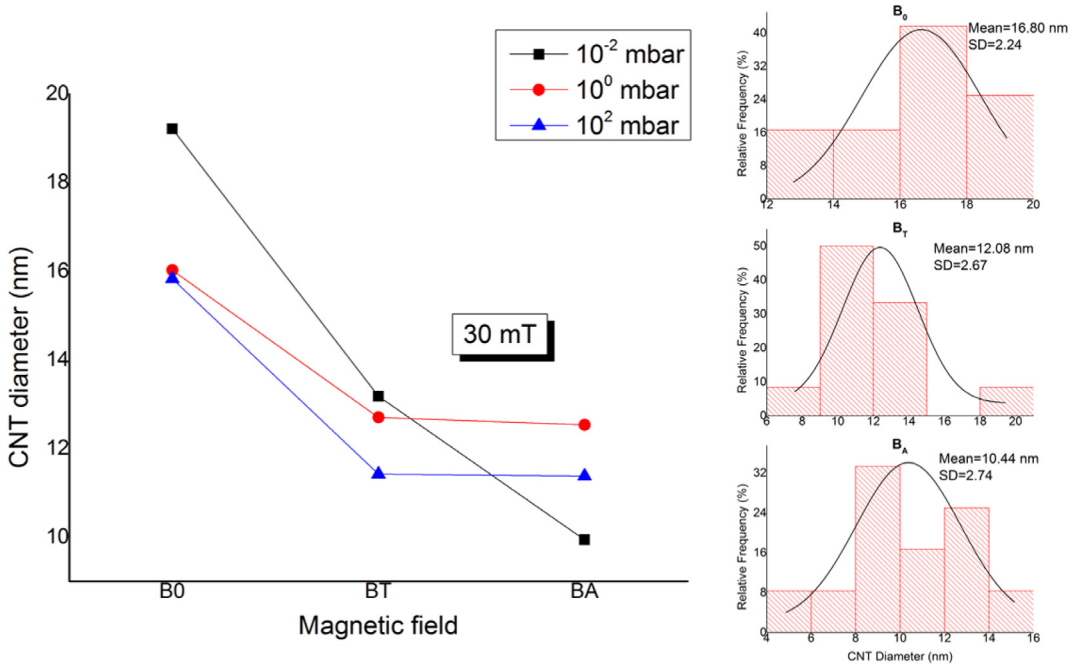

Fig. 3 MWCNTs' average diameter versus applied magnetic field configuration for Transverse magnetic field (B_T), Axial magnetic field (B_A) and absence of magnetic field in different ambient pressures measured by TEM.

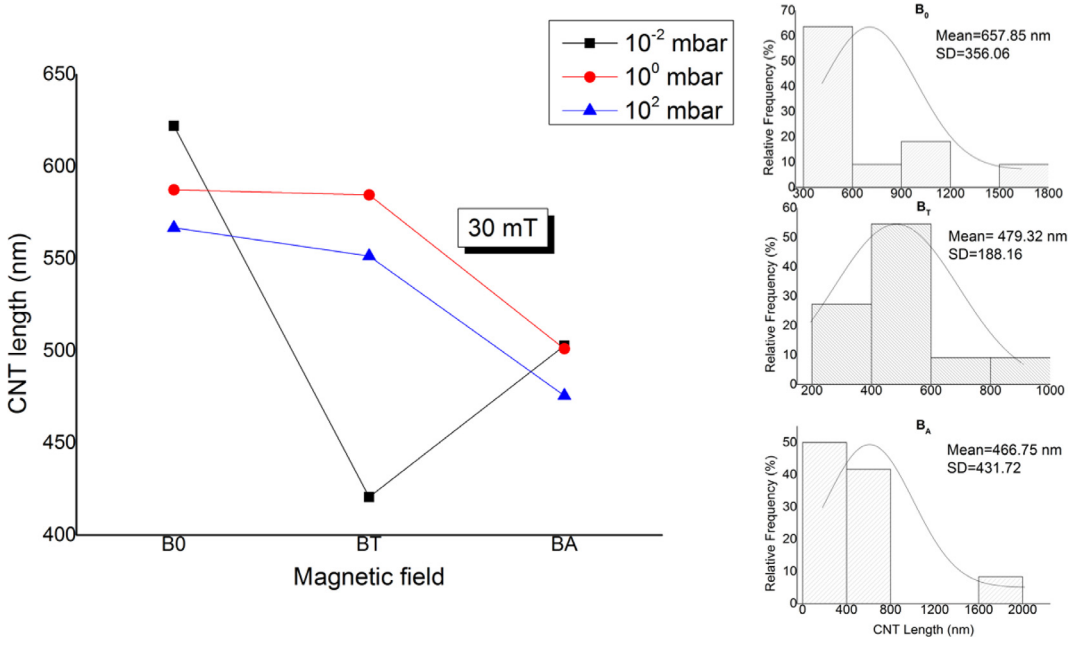

Fig. 4 MWCNTs' average length versus applied magnetic field configuration for Transverse magnetic field (B_T), Axial magnetic field (B_A) and absence of magnetic field in different ambient pressures measured by TEM.

results in a downshifted G band while compressive stress results in upshifted of Raman frequency. The downshift of G band is observed for CNTs synthesized under the influence of axial magnetic field B_T at ambient pressures of 1 and 10^{-1} mbar was from 1573 cm^{-1} to 1568 cm^{-1}. This downshift of G band indicates the increase in tensile stress resulting from elongation of tube structure. Alternatively, the intensity ratio between D and G bands (indicated by I_D/I_G) represents the level of defects in tube structure. Low I_D/I_G indicates tube structure growth with fewer defects while a high intensity ratio is indicative of high level of defects in tube structure. Fig. 7 shows the trend of I_D/I_G ratio for different magnetic configurations applied and under different ambient pressures. As illustrated in the Fig. 7, CNTs synthesized in the absence of magnetic field, B_0 have shown a gradual increase in I_D/I_G ratio as ambient pressure is increased from 10^{-2} to 10^2 mbar. In

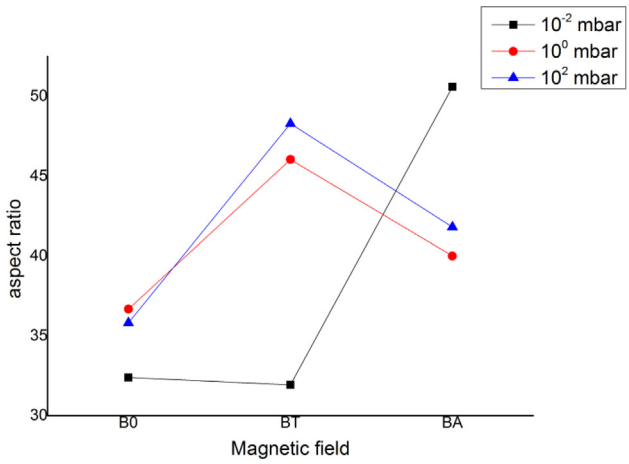

Fig. 5 CNT aspect ratio for different applied magnetic field configurations and ambient pressure.

contrast, in case of applied transverse magnetic field B_T, the I_D/I_G ratio is decreased steeply as ambient pressure rose from 10^{-2} to 10^2 mbar. This indicates a reduction in the tube structure defect level under applied transverse magnetic fields. In the presence of an axial magnetic field effect, B_A, the trend shows I_D/I_G ratio largely stabilized at a low level, although the results for ambient pressure 10^1 mbar show a high rise in defect level. A similar pattern is observed in the absence of magnetic field, B_0. The results show the influence of applied magnetic field on the arc discharge plasma in reducing the defect level of the resulting carbon nanotube structure.

Table 1 Raman features of CNTs samples for wavenumber from 1200^{-1} to 1800 cm^{-1}.

Magnetic field (30 mT)	Ambient pressure (mbar)	D band (cm^{-1})	G band (cm^{-1})	I_D/I_G
No Magnet applied	10^{-2}	1352	1580	0.26199
	10^{-1}	1330	1572	1.46315
	1	1355	1563	0.63152
	10^1	1355	1580	1.02909
	10^2	1348	1580	0.84214
Transverse magnetic field	10^{-2}	1344	1565	0.79463
	10^{-1}	1347	1579	0.53803
	1	1347	1580	0.73972
	10^1	1356	1583	0.60100
	10^2	1356	1580	0.15117
Axial Magnetic field	10^{-2}	1345	1579	0.39636
	10^{-1}	1339	1576	0.51341
	1	1337	1573	0.17515
	10^1	1331	1568	1.42381
	10^2	1337	1568	0.57893

Low values of full width half maximum (FWHM) in the G band are associated with MWCNT samples grown with improved of structural quality [27]. The results show that most of MWCNTs formed using this technique have good structural quality and low FWHM especially when the plasma discharge was conducted at a low pressure of 0.01 mbar. Wider G bands obtained at ambient pressure 0.1 mbar, which indicates a low structural quality of MWCNTs obtained which correlate with

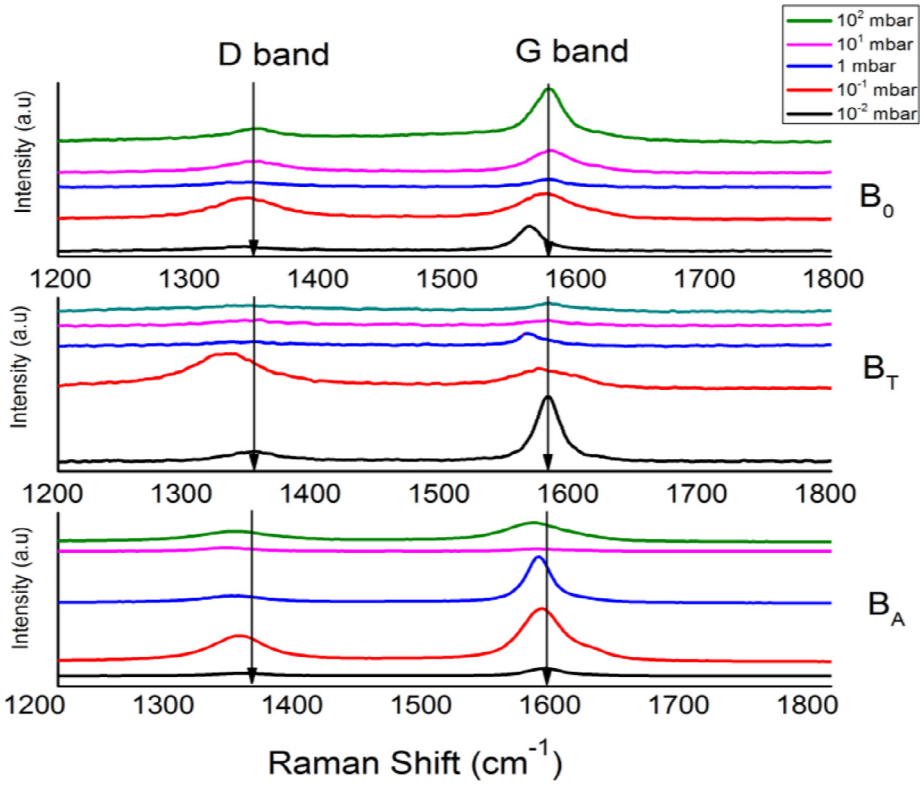

Fig. 6 Raman spectra for CNT sample synthesize in variant magnet configurations and ambient pressures.

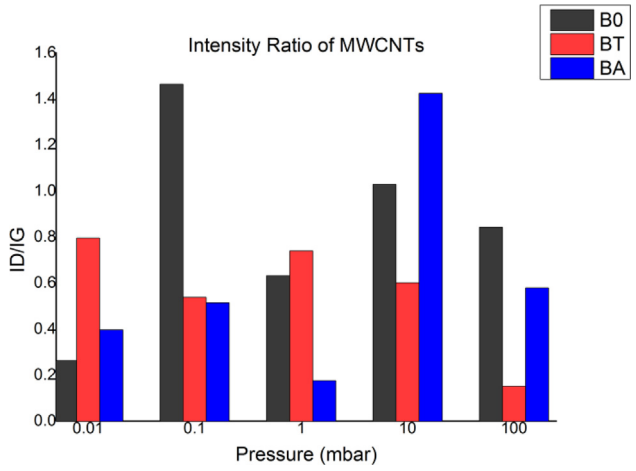

Fig. 7 I_D/I_G for MWCNT samples synthesized in variant magnetic field configurations and ambient pressures.

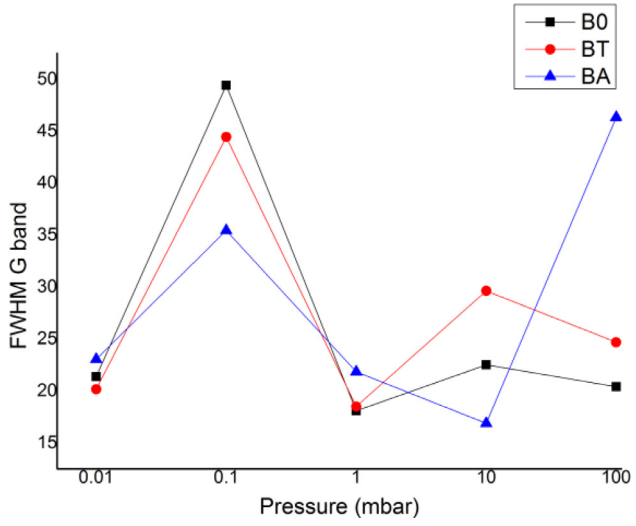

Fig. 8 Trend of FWHM of G-band in Raman spectra of MWCNT samples synthesized in variant magnetic field configurations and ambient pressures.

the rise in D band as shown in the Raman spectra denoted in Fig. 6 (indicated by the red line). However, the applied magnetic field at ambient pressure 0.1 mbar results in significantly higher structural quality of MWCNTs as indicated by FWHM in Fig. 8 compared with MWCNTs formed in the absence of magnetic field.

5. XRD and FTIR analysis

The X-Ray diffraction (XRD) is a spectroscopic technique that can be used to investigate the crystal properties of carbon nanotube structure. The repeatable atomic arrangement referred to as crystal structure diffracts the X-ray beam resulting in increased peak intensity at specified diffraction angles (2θ) related to the specific lattice of the crystal structure. In this case, the XRD spectra shown in Fig. 9 depicts strong peaks at a diffraction angle of 26°, which represents diffraction by the basal plane (0 0 2) from the atomic graphite layer (ref no JCPDS no. 75-1621) [28]. The plane (0 0 2) refers to the graphene layer rolled to form carbon nanotubes structure. The shifting of the X-Ray diffraction angle permits inference of the interlayer distance of the MWCNTs measured based on common Bragg equation:

$$n\lambda = 2d\sin\theta \tag{1}$$

where n is an integer referring to the order of diffracted beam, λ is the wavelength of X-rays (1.54 Å), θ refers to the diffracted angle and d is the spacing between graphene interlayer, referred to as the d_{002} spacing. Table 2 outlines the analysis data obtained from XRD spectra of MWCNT samples synthesized in different ambient pressures and magnetic configurations.

Referring to Fig. 9, the XRD spectra show that the crystallinity of MWCNTs grown in the absence of magnetic field increases with increase in ambient pressure from 10^{-2} to 10^{2} mbar as indicated by the rise in peak (0 0 2) intensity as shown in Fig. 9(a). A similar trend is observed for samples grown under applied axial magnetic fields. Meanwhile, MWCNTs grown under transverse magnetic fields demonstrate moderate crystallinity for the plane (0 0 2) intensity detected to be maintained for all applied ambient pressures. The angular shift of

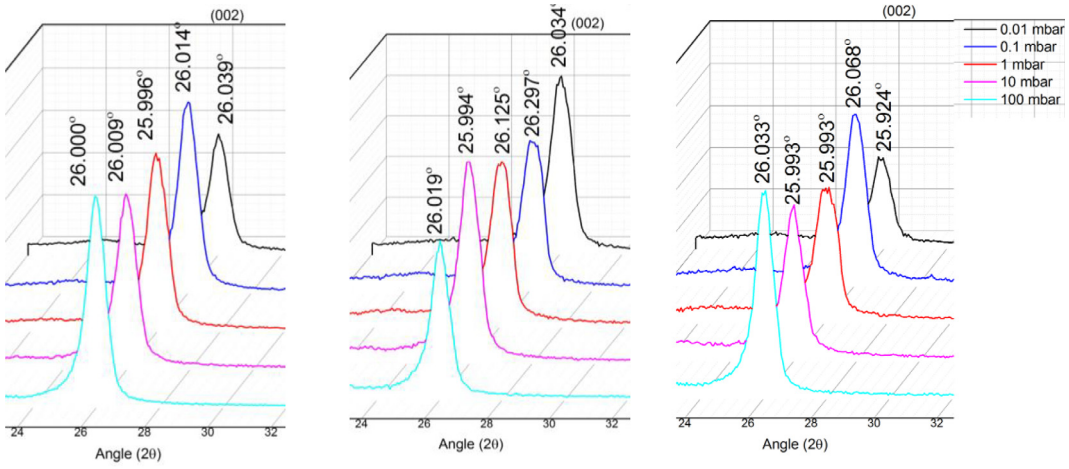

Fig. 9 XRD spectra of CNTs synthesized under variable ambient pressures and magnetic field configurations (a) absence of magnetic field (b) transverse magnetic field and (c) axial magnetic field.

Table 2 XRD details of MWCNTs synthesized under transverse and axial magnetic field configuration at ambient pressure ranging from 10^{-2} to 10^{2} mbar.

Magnetic Field (30 mT)	Ambient pressure (mbar)	2θ (°)	d_{002} (Å)	Crystallite size (nm)	Crystallite size/d_{002}	CNT walls
No Magnet applied	10^{-2}	26.0388	3.42211	12.5053	36.57750	18.2887
	10^{-1}	26.0136	3.42537	11.6456	34.03061	17.0153
	1	25.9963	3.42761	11.3238	33.06854	16.5342
	10^{1}	26.0092	3.42594	11.4669	33.50263	16.7513
	10^{2}	26.0004	3.42708	12.3211	35.98635	17.9931
Transverse magnetic field	10^{-2}	26.0342	3.42271	11.1078	32.48430	16.2421
	10^{-1}	26.2971	3.38908	10.7166	31.65106	15.8255
	1	26.1252	3.41099	10.5220	30.87692	15.4384
	10^{1}	25.9942	3.42789	10.9190	31.88523	15.9426
	10^{2}	26.0187	3.42472	12.5698	36.73832	18.3691
Axial Magnetic field	10^{-2}	25.9243	3.43697	12.8398	37.39351	18.6967
	10^{-1}	26.0681	3.41833	11.9195	34.90264	17.4513
	1	26.0866	3.41595	10.2849	30.13729	15.0686
	10^{1}	25.9930	3.42804	12.6332	36.88776	18.4438
	10^{2}	26.0326	3.42291	12.6732	37.06003	18.5300

2θ indicates the change of plane (0 0 2) interlayer space as discussed earlier. As calculated using equation (1), the d_{002}-spacing of MWCNTs is maintained at 3.425 Å in the absence of transverse magnetic field, whereas in presence of a transverse magnetic field, the MWCNTs grow with a smaller d_{002} spacing of 3.414 Å, while in the presence of an axial magnetic field, the d_{002} spacing is measured maintained at 3.424 Å as an average, which is slightly smaller than that of crystalline graphite (3.53 Å) [29].

The crystallite size, L_{002} is calculated by from FWHM using the Debye–Scherer formula with a constant K for spherical crystal cubic symmetry [30]:

$$L_{002} = \frac{K\lambda}{B(\theta)\cos\theta} \tag{2}$$

where λ is the wavelength, θ is the diffracted angle, and B is FWHM. By dividing the number of stacking graphite crystallites L_{002} by the d_{002} spacing, the number of walls in formed by carbon nanotubes can be estimated [31] as illustrated in Fig. 10. However, MWCNTs consist of tubular structure formed by growth of multiple graphene layers, thus dividing crystallites L_{002} by the d_{002} spacing will only shows total layers formed under the radial cross section of MWCNTs. Therefore,

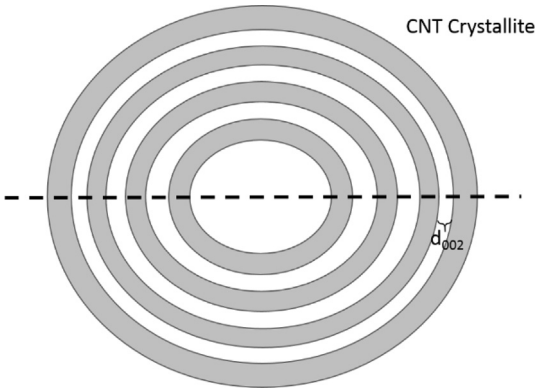

Fig. 10 Cross section of crystallite carbon nanotube radial tube structure.

the actual number of layers formed by CNTs could be approximated by the formula.

$$\text{CNT walls} = 0.5\left(\frac{L_{002}}{d_{002}}\right) \tag{3}$$

Fig. 11 shows the trend of MWCNT wall for variations in pressure and magnetic field configuration calculated from the XRD data. These data are supported by HRTEM micrographs of MWCNT layers as shown in Fig. 11(b). The trend of CNT walls shows higher wall formation under a low pressure of 10^{-2} mbar. The number of walls decreased as the pressure increased to 1 mbar. As the ambient pressure increased to 10^{2} mbar, the number of nanotube walls increased again in range of 18–19 walls. The synthesis of MWCNTs under an axial magnetic field (indicated by the blue line in Fig. 11) grows a larger number of nanotube walls as compared to the absence of magnetic field. In the presence of a transverse magnetic field (indicated by the red line), the number of tube walls is significantly reduced. The graph infers that the number of MWCNT walls can be regulated by varying applied magnetic field and configuration.

Fourier transform Infra-red Spectroscopy (FTIR) was employed to characterize bonding exhibited by grown CNTs. The FTIR studies on MWCNTs [26] were performed using a Perkin Elmer FTIR machine where the results are depicted in Fig. 12. The pellets are prepared by mixing CNTs with KBr. The CNT samples were scanned ten times using a spectral range from 450 cm^{-1} to 4000 cm^{-1}. The peak in the region 1430–1650 cm^{-1} corresponds to C=C stretching of MWCNT, whereas the peak at 1560 cm^{-1} represents the stretching vibration of C=C [32]. The peak at 1564 cm^{-1} is associated with the skeletal vibrational of graphene sheets [33]. The peak at 1637 cm^{-1} also corresponds to C=C stretching vibration [34]. In an air ambient environment, the results show rise in peak at position 1450 cm^{-1} in Fig. 12(a) indicating an increase in growth of MWCNTs with decrease in ambient pressure from 10^{2} to 10^{-2} mbar. This result is in agreement with the FESEM analysis which shows an increase in MWCNT diameter and length as ambient pressure decreased to 10^{-2} mbar. In the presence of transverse magnetic field, the intensity of peak at 1450 cm^{-1}

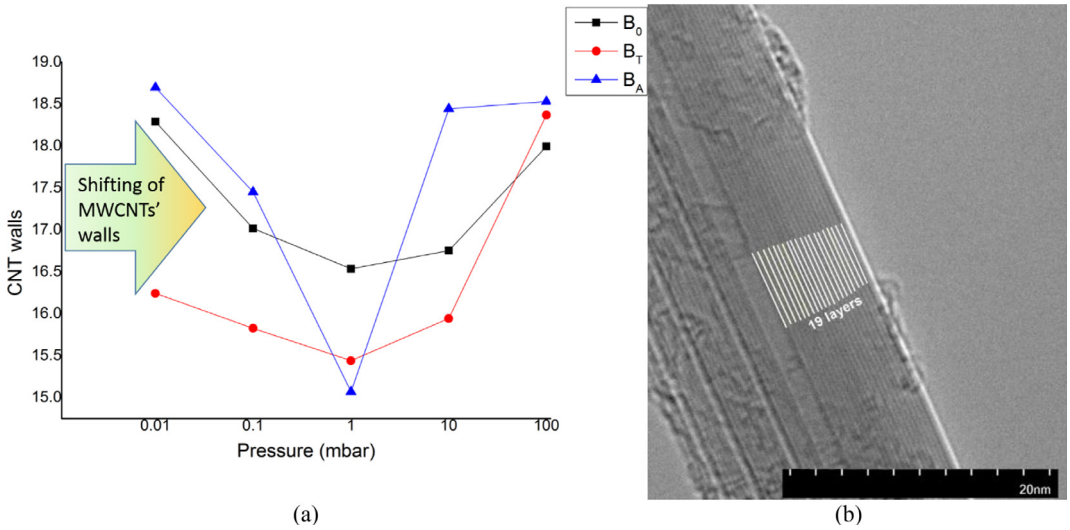

Fig. 11 Number of walls of MWCNTs (a) calculated based on XRD data synthesized in different ambient pressure and magnetic configuration and (b) HRTEM micrograph under axial magnetic field at pressure 10^{-2} mbar.

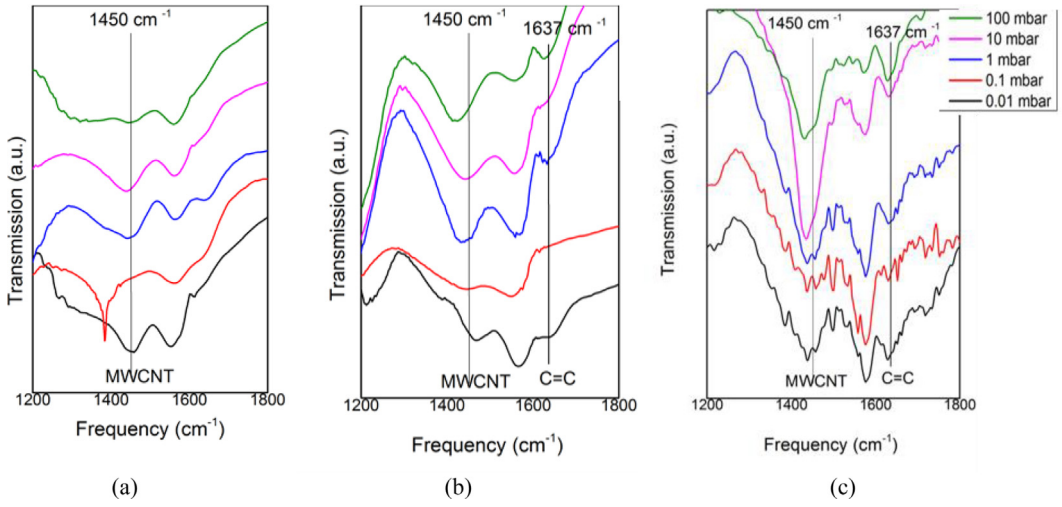

Fig. 12 FTIR spectra of MWCNTs synthesized under variable ambient pressure and magnetic configuration (a) absence of magnetic field (b) transverse magnetic field and (c) axial magnetic field.

corresponds to stronger stretching vibrations is increased with an increase in ambient pressure from 10^{-2} to 10^{2} mbar. In the presence of axial magnetic field, the trend of FTIR spectra shows an increase in intensity for peak 1450 cm^{-1} as ambient pressure increased from 10^{-2} to 10^{1} mbar as shown in Fig. 12(c). It is observed from FTIR spectra that a strong absorption peak at 1637 cm^{-1} attributed to C = C stretching vibration appears in the presence of external transverse and axial magnetic fields during synthesis of MWCNTs. This shows increased chemical stability as the C=C bonding in MWCNTs is strengthened by the influence of magnetic fields applied during the growth of MWCNTs in arc discharge plasma.

The comparison of this study with other research work done is presented in Table 3. Volotskova et al. have applied customized magnetic field to create different plasma temperature and density regions thus induce different growth zone and eventually separate CNTs with other nanomaterials [35]. Zhang et al. applied magnetic field 10G to separate CNTs with different diameter synthesized by altering the position of magnet within plasma [36]. Keidar et al. have applied magnetic field to enhance CNT growth and increase the length of SWCNTs [37] by creating strong plasma confinement and increase plasma density therefore increase carbon ion flux to catalyst surface during growth process and create long CNT structure. Volotskova et al. have reported successful fabrication of controlled growth of SWCNTs with different chiralities and diameters [38]. In present study, the number of walls can potentially being controlled by applying magnetic field.

6. Summary

In summary, a straightforward magnetic field assisted arc discharge plasma technique used to synthesize MWCNTs has

Table 3 The effect of magnetic field on the growth of CNTs structure.

Method to synthesis	Magnetic field strength	Background precursor gas	Ambient pressure	Catalyst	Major observation	Ref
Arc Discharge Plasma	30 mT (Axial and Transverse)	Air	10^{-2}–10^{2} mbar	No Catalyst	Shifting Number of CNTs' Walls formed	This Work
Arc Discharge Plasma	1.2 kG (Transverse)	He	500 Torr	Y/Ni	Separation of CNTs with other nanostructure	[35]
Arc Discharge Plasma	10 G (Transverse)	Ar-H_2	30 kPa	Fe/Mo	Diameter Control of CNTs Growth	[36]
Arc Discharge Plasma	0.4 T (Axial)	He	500–700 Torr	Y/Ni	Increase the length of CNTs	[37]
Arc Discharge Plasma	0.2–2 kG (Transverse)	He	300–500 Torr	Y/Ni	Tuning the distribution of CNTs formation	[38]

been successfully tested. MWCNTs grown by the arc discharge process are highly crystalline and have a fine, straight structure. The aspect ratio of MWCNTs could increase twofold with the application of an external magnetic field and the number of CNT walls potentially being regulated by external magnetic field effect. The intensity ratios of MWCNTs are decreased, showing a reduction in structural defects and an increase in graphitic structure when MWCNTs are grown under transverse and axial magnetic fields. Furthermore, mean crystallite size is reduced to few nm with an increase in ambient pressure from 10^{-2} to 1 mbar. Moreover, the number of nanotube walls is estimated from XRD data which is increased with a rise in ambient pressure from 1 to 10^{2} mbar. In addition, the FTIR spectra show increased chemical stability with the second peak rise at 1637 cm^{-1} corresponding to C=C stretching vibration in samples grown with the assistance of magnetic fields. Future work will focus on process optimization and control for the synthesis of high quality MWCNTs with growth of controlled number of walls that promotes unique electrical conductivity, flexibility, excellent electrocatalytic activity and mechanical integrity for vast possible applications including transparent electrodes, lightweight display panel, and flexible solar cells.

Acknowledgments

We would like to thank Universiti Teknologi Malaysia (UTM) for providing facilities and Ministry of Education Malaysia for financial support under MyBrain-15. This research project has been supported under Grant Tier-1 U929.

Conflict of interest statement

The authors declare that they have no conflict of interest.

References

[1] N. Behabtu, C.C. Young, D.E. Tsentalovich, O. Kleinerman, X. Wang, A.W. Ma, et al, Strong, light, multifunctional fibers of carbon nanotubes with ultrahigh conductivity, Science 339 (2013) 182–186.

[2] H. Badjian, A.R. Setoodeh, Improved tensile and buckling behavior of defected carbon nanotubes utilizing boron nitride coating – A molecular dynamic study, Phys. B Condens. Matter 507 (2017) 156–163.

[3] L. Lascialfari, P. Marsili, S. Caporali, M. Muniz-Miranda, G. Margheri, A. Serafini, et al, Carbon nanotubes/laser ablation gold nanoparticles composites, Thin Solid Films 569 (2014) 93–99.

[4] H. Pan, X. Yin, J. Xue, L. Cheng, L. Zhang, The microstructures, growth mechanisms and properties of carbon nanowires and nanotubes fabricated at different CVD temperatures, Diamond Related Mater. 72 (2017) 77–86.

[5] M.Y. Lone, A. Kumar, S. Husain, M. Zulfequar, Harsh, M. Husain, Growth of single wall carbon nanotubes using PECVD technique: An efficient chemiresistor gas sensor, Phys. E: Low-dimension. Syst. Nanostruct. 87 (2017) 261–265.

[6] S. Khorrami, R. Lotfi, Influence of carrier gas flow rate on carbon nanotubes growth by TCVD with Cu catalyst, J. Saudi Chem. Soc. 20 (2016) 432–436.

[7] J. Kennedy, F. Fang, J. Futter, J. Leveneur, P.P. Murmu, G.N. Panin, et al, Synthesis and enhanced field emission of zinc oxide incorporated carbon nanotubes, Diamond Related Mater. 71 (2017) 79–84.

[8] M. Keidar, A.M. Waas, On the conditions of carbon nanotube growth in the arc discharge, Nanotechnology 15 (2004) 1571.

[9] E.T. Thostenson, Z. Ren, T.-W. Chou, Advances in the science and technology of carbon nanotubes and their composites: a review, Compos. Sci. Technol. 61 (2001) 1899–1912.

[10] M.S. Roslan, K.T. Chaudary, Z. Haider, M.S. Aziz, J. Ali, Multi-walled carbon nanotubes grow under low pressure hydrogen, air, and argon ambient by arc discharge plasma, Fullerenes Nanotubes Carbon Nanostruct. 25 (2017) 269–272.

[11] L. Li, F. Li, C. Liu, H.-M. Cheng, Synthesis and characterization of double-walled carbon nanotubes from multi-walled carbon nanotubes by hydrogen-arc discharge, Carbon 43 (2005) 623–629.

[12] H. Qiu, Z. Shi, L. Guan, L. You, M. Gao, S. Zhang, et al, High-efficient synthesis of double-walled carbon nanotubes by arc discharge method using chloride as a promoter, Carbon 44 (2006) 516–521.

[13] T. Hirofumi, Y. Miki, S. Tateki, I. Shigeo, Carbon nanotubes in cathodic vacuum arc discharge, J. Phys. D Appl. Phys. 33 (2000) 826.

[14] Y. Su, P. Zhou, J. Zhao, Z. Yang, Y. Zhang, Large-scale synthesis of few-walled carbon nanotubes by DC arc discharge in low-pressure flowing air, Mater. Res. Bull. 48 (2013) 3232–3235.

[15] K. Chaudhary, J. Ali, P. Yupapin, Growth of small diameter multi-walled carbon nanotubes by arc discharge process, Chin. Phys. B 23 (2014) 035203.

[16] R. Joshi, J. Engstler, P.K. Nair, P. Haridoss, J.J. Schneider, High yield formation of carbon nanotubes using a rotating cathode in open air, Diamond Relat. Mater. 17 (2008) 913–919.

[17] K.T. Chaudhary, Z.H. Rizvi, K.A. Bhatti, J. Ali, P.P. Yupapin, Multiwalled carbon nanotube synthesis using arc discharge with hydrocarbon as feedstock, J. Nanomater. 2013 (2013), 145-145.
[18] K. Kiani, Free vibration of in-plane-aligned membranes of single-walled carbon nanotubes in the presence of in-plane-unidirectional magnetic fields, J. Vib. Control 22 (2015) 3736–3766.
[19] S. Farhat, M. Lamy de La Chapelle, A. Loiseau, C.D. Scott, S. Lefrant, C. Journet, et al, Diameter control of single-walled carbon nanotubes using argon–helium mixture gases, J. Chem. Phys. 115 (2001) 6752–6759.
[20] D.V. Smovzh, I.A. Kostogrud, S.Z. Sakhapov, A.V. Zaikovskii, S.A. Novopashin, The synthesis of few-layered graphene by the arc discharge sputtering of a Si-C electrode, Carbon 112 (2017) 97–102.
[21] M. Keidar, I. Levchenko, T. Arbel, M. Alexander, A.M. Waas, K.K. Ostrikov, Magnetic-field-enhanced synthesis of single-wall carbon nanotubes in arc discharge, J. Appl. Phys. 103 (2008) 094318.
[22] J.T. Gudmundsson, A. Hecimovic, Foundations of DC plasma sources, Plasma Sources Sci. Technol. 26 (2017) 123001.
[23] S.N. Kharin, Mathematical model of the short arc phenomena at the initial stage, in: Electrical Contacts – 1997 Proceedings of the Forty-Third IEEE Holm Conference on Electrical Contacts, 1997, pp. 289–305.
[24] A. Anders, G.Y. Yushkov, Ion flux from vacuum arc cathode spots in the absence and presence of a magnetic field, J. Appl. Phys. 91 (2002) 4824–4832.
[25] S. Brown, A. Jorio, P. Corio, M. Dresselhaus, G. Dresselhaus, R. Saito, et al, Origin of the Breit-Wigner-Fano lineshape of the tangential G-band feature of metallic carbon nanotubes, Phys. Rev. B 63 (2001) 155414.
[26] M. Dresselhaus, P. Eklund, Phonons in carbon nanotubes, Adv. Phys. 49 (2000) 705–814.
[27] S. Osswald, M. Havel, Y. Gogotsi, Monitoring oxidation of multiwalled carbon nanotubes by Raman spectroscopy, J. Raman Spectrosc. 38 (2007) 728–736.
[28] Z. Wang, D. Ba, F. Liu, P. Cao, T. Yang, Y. Gu, et al, Synthesis and characterization of large area well-aligned carbon nanotubes by ECR-CVD without substrate bias, Vacuum 77 (2005) 139–144.
[29] H. Dai, X. Gao, E. Liu, Y. Yang, W. Hou, L. Kang, et al, Synthesis and characterization of graphitic carbon nitride sub-microspheres using microwave method under mild condition, Diamond Related Mater. 38 (2013) 109–117.
[30] R. Das, S. Bee Abd Hamid, E. Ali, S. Ramakrishna, W. Yongzhi, Carbon nanotubes characterization by X-ray powder diffraction–a review, Curr. Nanosci. 11 (2015) 23–35.
[31] S. Faraji, K. Stano, C. Rost, J.-P. Maria, Y. Zhu, P.D. Bradford, Structural annealing of carbon coated aligned multi-walled carbon nanotube sheets, Carbon 79 (2014) 113–122.
[32] X.-L. Ling, Y.-Z. Wei, L.-M. Zou, S. Xu, Preparation and characterization of hydroxylated multi-walled carbon nanotubes, Colloids Surfaces A Physicochem. Eng. Aspects 421 (2013) 9–15.
[33] W. Zeng, G. Zhang, S. Hou, T. Wang, H. Duan, Facile synthesis of Graphene@ NiO/MoO 3 composite nanosheet arrays for high-performance supercapacitors, Electrochim. Acta 151 (2015) 510–516.
[34] Y. Wang, L. Chen, Analysis of malachite green in aquatic products by carbon nanotube-based molecularly imprinted–matrix solid phase dispersion, J. Chromatogr. B 1002 (2015) 98–106.
[35] O. Volotskova, I. Levchenko, A. Shashurin, Y. Raitses, K. Ostrikov, M. Keidar, Single-step synthesis and magnetic separation of graphene and carbon nanotubes in arc discharge plasmas, Nanoscale 2 (2010) 2281–2285.
[36] Y. Su, Y. Zhang, H. Wei, Z. Yang, E.S.-W. Kong, Y. Zhang, Diameter-control of single-walled carbon nanotubes produced by magnetic field-assisted arc discharge, Carbon 50 (2012) 2556–2562.
[37] M. Keidar, I. Levchenko, T. Arbel, M. Alexander, A.M. Waas, K. Ostrikov, Increasing the length of single-wall carbon nanotubes in a magnetically enhanced arc discharge, Appl. Phys. Lett. 92 (2008) 043129.
[38] O. Volotskova, J.A. Fagan, J.Y. Huh, F.R. Phelan Jr, A. Shashurin, M. Keidar, Tailored distribution of single-wall carbon nanotubes from arc plasma synthesis using magnetic fields, ACS Nano 4 (2010) 5187–5192.